NASA
Technical
Paper
2191

August 1983

Vector-Algebra Approach To Extract Denavit-Hartenberg Parameters of Assembled Robot Arms

L. Keith Barker

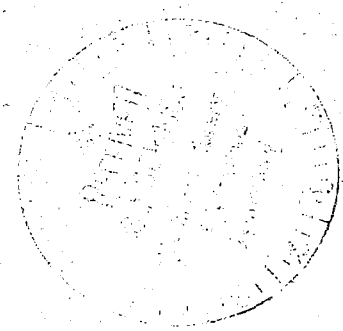

25th Anniversary
1958-1983

NASA

NASA
Technical
Paper
2191

1983

Vector-Algebra Approach To Extract Denavit-Hartenberg Parameters of Assembled Robot Arms

L. Keith Barker
Langley Research Center
Hampton, Virginia

NASA
National Aeronautics
and Space Administration

**Scientific and Technical
Information Branch**

SUMMARY

Transformation matrices from one joint axis system to another are used in the control of robot arms and in the passage of sensor information along the arms. The Denavit-Hartenberg parameters, which precisely describe the relative location of one joint axis system with respect to another, define the elements in these matrices. This paper presents a vector-algebra approach to extract the Denavit-Hartenberg parameters for any assembled robot arm.

Measurement data needed in the parameter-extraction process can be generated by varying the joint angles in a robot arm and measuring the location of a point on the robot hand (or other extension). The Denavit-Hartenberg parameters relating consecutive joint axis systems are then calculated with these data. The parameter-extraction method appears promising as a useful tool for researchers and may possibly be a useful industrial procedure.

INTRODUCTION

Researchers are currently trying to improve the control and design of robot arms and to add a certain degree of autonomy for future space applications, such as the service and repair of satellites (ref. 1). Commercially available (or prototype) robot arms are used to verify concepts, validate mathematical models, and realize operational problems. However, a difficulty arises in that parameters in the mathematical equations necessary to describe these arms are not always available or the supplied parameters are not sufficiently accurate for end-point control.

If an operator remotely controls the hand of a robot arm by commanding translational and rotational rates about the hand axis system, then these rates must be resolved mathematically into joint rates along the arm to effect these commands (resolved-rate control, ref. 2). This resolution depends on the location of the joints relative to each other. These locations are usually not available and are difficult to measure for assembled commercially available robot arms. But, in studies involving the control of these arms, this information is required.

Because researchers often use robot arms in a manner other than that for which they were originally intended (for example, some robot arms were not originally intended to be controlled in a teleoperator mode by resolved rate), necessary parameters are often not available for the requisite mathematical models. Moreover, certain parameters may represent proprietary information. Whatever the reason, there is a definite need for an accurate method to extract these parameters without having to disassemble the robot arms. Such a method may also prove useful in the extraction of a new set of definitive parameters to allow resumed control of a misaligned or bent robot arm, for example on a factory floor or in a space application of a rigid-body manipulator; via industrial enhancements, such a method may be useful in the routine factory calibration of robot arms.

The purpose of this paper is to develop a vector-algebra approach for calculating the relative joint geometry of an assembled robot arm. Specifically, the Denavit-Hartenberg parameters (ref. 3), which completely characterize this geometry, are calculated.

SYMBOLS

A_{i-1}^{i}	homogeneous transformation matrix from coordinate system i to $i - 1$
a_i	length of $\vec{a}_i$
$\vec{a}_i$	common normal vector between Z_{i-1} and Z_i
$\vec{C}_i$	vector from world coordinate system to center of circular trajectory of point F about line of rotation for joint i
F	point on extension attached to robot hand
i	integer to indicate different axis systems and associated parameters
K_i	constant defined by equation (6)
k	integer argument used to label corresponding measurement data
$\vec{\ell}_i$	vector from world coordinate system to general point on line of rotation for joint i
$\vec{\ell}_i^*$	vector from world coordinate system to point where $\vec{v}_i^*$ touches line of rotation for joint i
M	number of unit vectors $\vec{u}_i(k)$ to be averaged
O_i, O_w	origin of joint i and world axis system, respectively
$\vec{P}_i$	measured position vector in world coordinates to point F
$\vec{P}_i(k)$	measured vector $\vec{P}_i$ associated with measurement data set k
$Q(x,y,z)$	point in three-dimensional space
$\vec{R}_i$	position vector from origin of world coordinate system to origin of coordinate system i
r_i	length of $\vec{r}_i$; relative distance between coordinate systems $i - 1$ and i along Z_{i-1}
$\vec{r}_i$	vector along Z_{i-1} from origin of coordinate system $i - 1$ to tail of $\vec{a}_i$
$\vec{S}_i$	vector from world coordinate system to tail of vector $\vec{a}_i$ (see fig. 8)
$\vec{u}_i$	unit vector normal to plane of circular trajectory of point F and in direction of rotational vector $\vec{\omega}_i$
$\vec{u}_i(k)$	calculated unit vector $\vec{u}_i$ associated with measurement data set k
$\vec{v}_i$	vector drawn from point on line of rotation for joint i to point on line of rotation for joint $i + 1$
$\vec{v}_i^*$	vector $\vec{v}_i$ with minimum length; normal vector between lines of rotation for joints i and $i + 1$

X_i axis directed along common normal between Z_{i-1} and Z_i

X_w, Y_w, Z_w world coordinate axes

x_i, y_i, z_i coordinate along X_i, Y_i, and Z_i, respectively

x_w, y_w, z_w world coordinate along X_w, Y_w, and Z_w, respectively

Y_i axis directed to complete right-hand axis system with X_i and Z_i

Z_i axis of rotation of joint $i + 1$

α_i angle between Z_{i-1} and Z_i, measured positively (as shown in fig. 3) about positive X_i

β_i constant bias angle, which when summed with joint angle θ_i, yields joint angle θ_i'

θ_i joint angle with initial value corresponding to position of robot arm in figure 1

$\theta_i(k)$ joint angle θ_i associated with data set k

$\Delta\theta_i(k)$ incremental changes in joint angle $\theta_i(k)$

θ_i' joint angle between X_{i-1} and X_i, measured positively (as shown in fig. 3) about positive Z_{i-1}

λ_i real variable in vector line equation

λ_i^* value of λ_i which makes $\vec{v}_i$ normal to line of rotation of joint i

ρ_i radius of circular trajectory of point F about line of rotation for joint i

$\vec{\Omega}_i$ unit vector in direction of $\vec{u}_i \times \vec{u}_{i+1}$

$\vec{\omega}_i$ rotational velocity of joint i

Mathematical notations:

$\| \|$ length of vector

$\cdot$ dot or scalar product

$\times$ cross or vector product

ANALYSIS

A robot arm with rotational joints is depicted in figure 1. As shown by the inset of wrist motions in this figure, θ_4 corresponds to a rotation of the bottom of the wrist assembly mounted at the end of the arm, whereas θ_6 directly rotates and θ_5 tilts the cylindrical element (end effector) which is attached to the wrist. In reality, a mechanism which opens and closes is attached to the wrist for

manipulating objects. The robot arm in figure 1 is used for illustration, but the subsequent development is valid for any geometric configuration of robot arm.

Suppose the exact location and orientation of each joint axis system of the robot arm in figure 1 are not known. The objective in this analysis is to develop a method to determine the parameters which establish the geometric relationships among the joint axis systems for an assembled robot arm. This objective is accomplished by moving the arm to different positions and making certain measurements, which are later used in equations to extract the desired parameters.

Measurements

Joint angle measurements.- As a point of reference for joint angle measurements, define $\theta_i = 0$ $(i = 1, 2, \ldots, 6)$ for the initial position of the robot arm shown in figure 1. Thereafter, these joint angles are referenced to this initial zero position.

World coordinates.- The world reference axis system indicated in figure 2 is an arbitrarily fixed axis system. For example, the origin of this axis system may be located at the corner of a flat table upon which the robot arm is stationed, or the world axis system may correspond to the axis system of a laser transit or a camera. With respect to this world axis system, the rectangular coordinates (x_w, y_w, z_w) of the point F in figure 2 are obtained. The point F is located arbitrarily on some extension of the robot hand so that when a rotation occurs, by varying a joint angle θ_i, the point F will move to another position in the world coordinate space. It is not necessary to know the length or orientation of the extension.

The robot arm is moved to different positions by varying its joint angles. At each new position, the joint angles θ_i are available from sensors in the robot arm itself, whereas the location of point F is actually measured by using external measurement devices (sensors). It is assumed that measurements of joint angles θ_i and corresponding world coordinates of point F are available for the robot arm in different positions for this analysis. Before proceeding, the axis systems to be established are described.

Joint Axis Systems

Figure 3 illustrates the axis systems associated with joints i and i + 1. By convention, joint i is associated with the coordinate system i - 1. Hence, joint i corresponds to the axis system with origin at O_{i-1}, whereas joint i + 1 corresponds to the other axis system with origin O_i. By definition, the axis of rotation for joint i always lies along the associated Z_{i-1}. The vector $\vec{a}_i$ is the normal vector between Z_{i-1} and Z_i, being directed toward Z_i. The intersection point of $\vec{a}_i$ with Z_i locates the origin O_i. The axis X_i originates from O_i in the same direction as $\vec{a}_i$. In the event that Z_{i-1} and Z_i intersect (fig. 3(b)), $\vec{a}_i$ is the zero vector, and X_i is then directed from this intersection in the direction of the cross product obtained by multiplying a unit vector along Z_{i-1} by a unit vector along Z_i. The vector $\vec{r}_i$ is the vector from the origin O_{i-1} to the intersection of $\vec{a}_i$ with Z_{i-1} (fig. 3(a)); for intersecting lines of rotation, $\vec{r}_i$ is a vector along Z_i from O_{i-1} to O_i (fig. 3(b)). The angle α_i is the angle between a line parallel to Z_{i-1} through the origin O_i and Z_i, being measured positive about positive X_i (fig. 3). Finally, the joint

angle θ_i' is the angle between X_{i-1} and a line parallel to X_i through O_{i-1} and is measured positive about positive Z_{i-1} (fig. 3). The axes Y_i and Y_{i-1}, which simply complete right-hand axis systems, are not shown for clarity.

The lengths of $\vec{a}_i$ and $\vec{r}_i$ are denoted by a_i and r_i. The relative joint parameters a_i, r_i, and α_i and the joint angle θ_i are referred to as the Denavit-Hartenberg parameters (ref. 2) and completely characterize the relative joint geometry.

Basic coordinate transformation.- The relative joint geometry dictates the basic transformation equations between adjacent joints. The coordinates of a point $Q(x,y,z)$ with respect to the coordinate system i in figure 3 can be transformed to coordinates of Q with respect to the coordinate system $i - 1$ by the relation:

$$\begin{bmatrix} x \\ y \\ z \\ 1 \end{bmatrix}_{i-1} = A_{i-1}^{i} \begin{bmatrix} x \\ y \\ z \\ 1 \end{bmatrix}_{i} \tag{1}$$

with

$$A_{i-1}^{i} = \left[\begin{array}{ccc|c} \cos\theta_i' & -\cos\alpha_i \sin\theta_i' & \sin\alpha_i \sin\theta_i' & a_i \cos\theta_i' \\ \sin\theta_i' & \cos\alpha_i \cos\theta_i' & -\sin\alpha_i \cos\theta_i' & a_i \sin\theta_i' \\ 0 & \sin\alpha_i & \cos\alpha_i & r_i \\ \hline 0 & 0 & 0 & 1 \end{array}\right] \tag{2}$$

where A_{i-1}^{i} is the homogeneous transformation matrix from coordinate system i to $i - 1$ (ref. 4, for example). This basic transformation matrix, whose elements are defined by the Denavit-Hartenberg parameters, is used in controlling a robot arm and in transforming sensor signals along the arm.

Relationship between joint angles θ_i and θ_i'.- If the convention in figure 3 were used to define axis systems for the robot arm in figure 1, the joint angles would be θ_i' ($i = 1, 2, \ldots, 6$). In general, the joint angle θ_i' is not equal to the joint angle θ_i, which is referenced to the initial condition of the robot arm in figure 1. At this time, θ_i is measurable, but θ_i' is not measurable because the axis systems have not yet been established. Corresponding values of θ_i and θ_i'

result from application of the subsequent parameter extraction equations, and if required, a nonlinear relationship could be formed. However, most often, this functional relationship is adequately described by the linear equation:

$$\theta_i' = \theta_i + \beta_i \tag{3}$$

where β_i is a constant bias, reflecting an initial offset in θ_i'. Hence, if a calculated value of θ_i' corresponds to a measured value of θ_i, then β_i is calculated by using these values in equation (3).

Problem Statement

Given the world coordinate system in figure 4, let the location of the point O_{i-1} and the direction of X_{i-1} be known. Now, with joint angles θ_i and corresponding locations of point F (fig. 2), calculate the Denavit-Hartenberg parameters a_i, α_i, and r_i, and the joint angle θ_i'. Furthermore, find the origin O_i of the next axis system, which is located somewhere on the dashed line for $\vec{\omega}_{i+1}$, and the direction of X_i. The process is then repeated to establish subsequent axis systems. To initiate the process, use the origin O_w and the direction of X_w which are specified.

Circular Trajectory of Point F

In figure 2, let θ_1 vary and the remaining θ_i be fixed. Then, the point F on the robot arm will generate a circular trajectory about Z_0. In general, as θ_i varies, the point F will generate a circular trajectory about Z_{i-1}. For a value of θ_i, the location of point F in world coordinates can be measured (for example, see appendix A).

Center of circular trajectory.- Figure 5 shows the circular trajectory of point F caused by changing θ_i (where $\|\vec{\omega}_i\|$ is the time derivative of θ_i). The vector $\vec{P}_i(k)$ gives the position of F in world coordinates when θ_i has the value $\theta_i(k)$, where k has been introduced to label corresponding data. The center of the circular trajectory in figure 5 is given by the constant vector $\vec{C}_i$. The components of this vector are computed by forming the dot product:

$$(\vec{P}_i(k) - \vec{C}_i) \cdot (\vec{P}_i(k) - \vec{C}_i) = \rho_i^2 \tag{4}$$

which can also be expressed as

$$\vec{C}_i \cdot \vec{P}_i(k) + K_i = \vec{P}_i(k) \cdot \vec{P}_i(k)/2 \tag{5}$$

where

$$K_i = -\left(\vec{C}_i \cdot \vec{C}_i - \rho_i^2\right)\Big/2 \tag{6}$$

is a constant.

Equation (5) represents k linear equations in four unknowns: K_i and the three components of the vector $\vec{C}_i$. Four different position vectors ($\vec{P}_i(k)$, k = 1, 2, 3, and 4) are sufficient to provide enough equations for the solution of these constants. Thus, a robot arm with 6 rotational joints would require 24 position measurements (4 for each of the 6 joints). Each position vector is made up of three components, representing a point in the world coordinate system (x_w, y_w, z_w). In actual situations, where sensor errors are present, more measurements will be needed to allow least-squares estimates of the constants.

Once the vector $\vec{C}_i$ and the scalar K_i are found, the radius of the circle is given by equation (6), written as

$$\rho_i = \sqrt{\vec{C}_i \cdot \vec{C}_i + 2K_i} \tag{7}$$

Unit vector $\vec{u}_i$.- Figure 6 shows the circular trajectory of point F and two position vectors $\vec{P}_i(k)$ and $\vec{P}_i(k+1)$, along with the incremental joint angle

$$\Delta\theta_i(k) = \theta_i(k+1) - \theta_i(k) \tag{8}$$

between these position vectors. A unit vector normal to the plane of the circular trajectory and passing through point C_i (whose coordinates are the components of the vector $\vec{C}_i$) is

$$\vec{u}_i(k) = \frac{\left[\vec{P}_i(k) - \vec{C}_i\right] \times \left[\vec{P}_i(k+1) - \vec{C}_i\right]}{\rho_i^2} \tag{9}$$

With $0 < \Delta\theta_i(k) \leq \pi$, $\vec{u}_i(k)$ in equation (9) is in the same direction as the rotational vector $\vec{\omega}_i$. An average $\vec{u}_i$ over M vectors

$$\vec{u}_i = \frac{1}{M} \sum_{k=1}^{M} \vec{u}_i(k) \tag{10}$$

should be used to reduce the effects of errors in actual measurements.

Lines of Rotation and Transverse Vector

Figure 7 shows lines of rotation for joints i and i + 1. Any point on the line of rotation for joint i is representable by the vector line equation

$$\vec{\ell}_i = \vec{C}_i + \lambda_i \vec{u}_i \tag{11}$$

Likewise, any point on the line of rotation for joint i + 1 is described by

$$\vec{\ell}_{i+1} = \vec{C}_{i+1} + \lambda_{i+1} \vec{u}_{i+1} \tag{12}$$

Define a transverse vector $\vec{v}_i$ between these lines of rotation as

$$\vec{v}_i = \vec{\ell}_{i+1} - \vec{\ell}_i \tag{13}$$

Parallel lines of rotation $\left(\vec{u}_i \times \vec{u}_{i+1} = 0;\ \vec{u}_i \cdot \vec{u}_{i+1} = \pm 1\right)$.- First of all, coincident lines of rotation for consecutive joints are not of interest because these joints are effectively one and not distinguishable. Therefore, in figure 7, for parallel lines,

$$\vec{C}_{i+1} - \vec{C}_i \neq 0 \tag{14}$$

For parallel lines of rotation, the point F in figure 2 generates circular trajectories in figure 7 which lie in the same plane; therefore,

$$\vec{v}_i^{*} = \vec{C}_{i+1} - \vec{C}_i \tag{15}$$

is normal to these lines and has a length equal to their distance of separation. Equation (15) is equation (13), with $\lambda_i = \lambda_{i+1} = 0$. Relocate $\vec{v}_i^{*}$ so that its initial point is the known location of the origin O_{i-1} on the line of rotation for joint i; that is,

$$\vec{\ell}_i^{*} = \vec{R}_{i-1} \tag{16}$$

where $\vec{R}_{i-1}$ is the vector from the world axis system to O_{i-1} (fig. 8). Then, the corresponding terminal point of $\vec{v}_i^{*}$ on the line of rotation for joint i + 1 is

$$\vec{\ell}_{i+1}^{*} = \vec{\ell}_i^{*} + \vec{v}_i^{*} \tag{17}$$

In effect, equation (16) reflects the assignment of $\vec{r}_i = 0$ to parallel lines of rotation.

Skew lines of rotation.- If the lines of rotation in figure 7 are not parallel, let λ_i^{*} and λ_{i+1}^{*} be those values of λ_i and λ_{i+1} in equations (11) and (12), respectively, which make $\vec{v}_i$ in equation (13) normal to the lines of rotation. Denote this vector $\vec{v}_i$ by $\vec{v}_i^{*}$. Then,

$$\vec{v}_i^{*} = \vec{\ell}_{i+1}^{*} - \vec{\ell}_i^{*} \tag{18}$$

where

$$\vec{\ell}_{i+1}^{*} = \vec{C}_{i+1} + \lambda_{i+1}^{*}\,\vec{u}_{i+1} \tag{19}$$

and

$$\vec{\ell}_i^{\,*} = \vec{C}_i + \lambda_i^* \vec{u}_i \tag{20}$$

are the intersection points of $\vec{v}_i^{\,*}$ with the lines of rotation. By definition of $\vec{v}_i^{\,*}$, two orthogonality conditions are

$$\vec{v}_i^{\,*} \cdot \vec{u}_i = 0 \tag{21}$$

and

$$\vec{v}_i^{\,*} \cdot \vec{u}_{i+1} = 0 \tag{22}$$

Equations (21) and (22) can be solved simultaneously for the scalar values λ_i^* and λ_{i+1}^* to get

$$\lambda_i^* = \frac{(\vec{C}_{i+1} - \vec{C}_i) \cdot [\vec{u}_i - (\vec{u}_{i+1} \cdot \vec{u}_i)\vec{u}_{i+1}]}{1 - (\vec{u}_{i+1} \cdot \vec{u}_i)^2} \tag{23}$$

and

$$\lambda_{i+1}^* = \frac{-(\vec{C}_{i+1} - \vec{C}_i) \cdot [\vec{u}_{i+1} - (\vec{u}_{i+1} \cdot \vec{u}_i)\vec{u}_i]}{1 - (\vec{u}_{i+1} \cdot \vec{u}_i)^2} \tag{24}$$

where, for skewed lines, $(\vec{u}_{i+1} \cdot \vec{u}_i) \neq 1$.

Relative Joint Geometry

In figure 8, $\vec{S}_i$ and $\vec{R}_i$ represent position vectors in world coordinates where $\vec{a}_i$ intersects the lines of rotation for joints i and $i + 1$. Thus,

$$\vec{S}_i = \vec{\ell}^*_i \tag{25}$$

$$\vec{R}_i = \vec{\ell}^*_{i+1} \tag{26}$$

$$\vec{a}_i = \vec{v}^*_i \tag{27}$$

$$\vec{r}_i = \vec{S}_i - \vec{R}_{i-1} \tag{28}$$

The direction of X_i is chosen to be either in the direction of $\vec{u}_i \times \vec{u}_{i+1}$ or $\vec{a}_i$. Conditions for these options are shown in table I and are dependent on the relationship between consecutive lines of rotation. Correspondingly consistent equations for determining θ_i' and α_i are shown in table II.

Equation for $\tan \theta_i'$.- All the equations for $\tan \theta_i'$ in table II have similar explanations; therefore, only consider

$$\tan \theta_i' = \frac{(\vec{a}_{i-1} \times \vec{a}_i) \cdot \vec{u}_i}{\vec{a}_{i-1} \cdot \vec{a}_i} \tag{29}$$

The numerator term in equation (29) shows the cross product of a vector $\vec{a}_{i-1}$ along X_{i-1} and a vector $\vec{a}_i$ along X_i and then forming the dot product of the result and a unit vector $\vec{u}_i$ along Z_{i-1} produces $\|\vec{a}_{i-1}\| \|\vec{a}_i\| \sin \theta_i'$ with the correct sign for a positive rotation about positive Z_{i-1} (or equivalently $\vec{u}_i$).

The denominator is $\|\vec{a}_{i-1}\| \|\vec{a}_i\| \cos \theta_i'$. Hence, the fraction represents $\tan \theta_i'$, where $0 \leq \theta_i' \leq 2\pi$. The joint angle θ_i' in equation (29) corresponds to the fixed position of joint i after $\vec{u}_i$ has been determined and joint $i + 1$ is being varied to obtain $\vec{u}_{i+1}$.

Tan α_i with X_i in direction of $\vec{a}_i$.- The appropriate equation in table II is

$$\tan \alpha_i = \left[(\vec{u}_i \times \vec{u}_{i+1}) \cdot \frac{\vec{a}_i}{\|\vec{a}_i\|} \right] \Big/ \vec{u}_i \cdot \vec{u}_{i+1} \tag{30}$$

The right-hand side of this equation shows the cross product of a vector along Z_{i-1} (or $\vec{u}_i$) and a vector along Z_i (or $\vec{u}_{i+1}$) and then the dot product of this result and a unit vector along X_i (or $\vec{a}_i/\|\vec{a}_i\|$) gives $\sin \alpha_i$. The dot product in the denominator yields $\cos \alpha_i$.

Tan α_i with X_i in direction of $\vec{u}_i \times \vec{u}_{i+1}$ when consecutive lines of rotation intersect.- Figure 9 shows the unit vector $\vec{u}_{i+1}$ along Z_i, the unit vector $\vec{u}_i$ along a line parallel to Z_{i-1}, and the angle α_i between these two vectors. A unit vector defined by

$$\vec{\Omega}_i = \frac{\vec{u}_i \times \vec{u}_{i+1}}{\|\vec{u}_i \times \vec{u}_{i+1}\|} \tag{31}$$

establishes the direction of X_i. Hence,

$$\tan \alpha_i = \frac{(\vec{u}_i \times \vec{u}_{i+1}) \cdot \vec{\Omega}_i}{\vec{u}_i \cdot \vec{u}_{i+1}} \tag{32}$$

is the ratio of $\sin \alpha_i$ to $\cos \alpha_i$. Or, equivalently,

$$\tan \alpha_i = \frac{\|\vec{u}_i \times \vec{u}_{i+1}\|}{\vec{u}_i \cdot \vec{u}_{i+1}} \tag{33}$$

which is shown in table II.

Calibration of Joint Angles

The joint angle θ_i' can be calibrated as follows. After positional data $\vec{P}_i(k)$ are obtained for variations in the joint angle θ_i, let θ_i^* be the fixed value of θ_i when the next positional data $\vec{P}_{i+1}(k)$ are collected for variations in θ_{i+1}. Moreover, let $(\theta_i')^*$ be the value of θ_i' that is computed with the positional data in the parameter extraction procedure. Then, $(\theta_i')^*$ corresponds to θ_i^*. If the functional relationship between θ_i and θ_i' is the linear equation (3), then

$$\beta_i = (\theta_i')^* - \theta_i^* \tag{34}$$

Thereafter, with this value of β_i, equation (3) gives θ_i' for different values of θ_i.

Extraction of the Denavit-Hartenberg parameters allows the definition of joint axis systems for the robot arm, such as those depicted in figure 10. The procedure in this analysis applies not only to robot arms but also to other jointed mechanisms. In addition, errors are not propagated. Although only rotational joints are discussed in the text, translational or sliding joints are easily handled as indicated in appendix B.

CONCLUDING REMARKS

A vector-algebra method is developed to extract the relative joint geometry (Denavit-Hartenberg parameters) of a robot arm or other jointed mechanisms. The only measurements required are the locations of a point on the robot hand for different joint angles. A minimum of four locations (i.e., world coordinates for four locations of the point) is required; however, more points should be used to reduce the effects of measurement errors. The robot arm is positioned by changing a set of joint angles (which are referenced to an arbitrarily specified zero position), and then the location of a point on the robot hand is measured with respect to a fixed world axis system (which is also arbitrarily specified). These positions and joint angles are used in equations to extract the relative joint parameters. More specifically, trajectories generated by a point on the robot arm (circular trajectory for rotational joints and line trajectory for sliding joints) and obtained by individual joint movements provide sufficient information to determine unit vectors along the lines of rotation or translation and to subsequently extract the Denavit-Hartenberg parameters.

This method for extracting relative joint geometry of robot arms will be useful to researchers who need these data for existing robot arms for either validation of mathematical models or for studies involving the actual control of these devices. This method, which does not require the robot arm to be disassembled, may also be useful in the recalibration of a misaligned or bent robot arm and, if sufficiently accurate, could become a useful industrial procedure. A merit of the method is that errors are not propagated.

Langley Research Center
National Aeronautics and Space Administration
Hampton, VA 23665
July 11, 1983

APPENDIX A

WORLD COORDINATES OF POINT F BY SINGLE SIGHTING DEVICE

The symbols used in this appendix are defined as follows:

d	distance from origin of world axis system to point F
F	point associated with robot arm; center of sphere
x_w, y_w, z_w	world coordinates
$\gamma, \gamma_1, \gamma_2$	elevation angles of sighting device
γ_{max}	elevation angle such that if line of sight is lowered sufficiently, it will pass through center of sphere
ρ_s	known sphere radius
ϕ	azimuth angle of sighting device

The parameter-extraction method presented in the text uses the world coordinates of a point F on the robot arm as input data. There are several ways to gather this information, with some ways being more accurate than others.

A technique which might be useful in obtaining the world coordinates of a point F is shown in figure A1. Since point F is somewhat arbitrary, consider it to be the center of a sphere of known radius ρ_s on an extension that is held by the robot hand. For reference, an arbitrary reference point is selected so that when it is sighted, the azimuth angle ϕ and elevation angle γ of the transit are considered to be zero. Now, ϕ is increased by changing γ until a line-of-sight tangent to the sphere is produced at $\gamma = \gamma_2$. With ϕ constant, γ is then reduced to $\gamma = \gamma_1$ which corresponds to the other line-of-sight tangent. The desired elevation angle γ_2 is the maximum elevation angle γ_{max} which exists as ϕ is increased, as indicated in figure A2. With these line-of-sight angles, the distance to point F is

$$d = \frac{\rho_s}{\sin\left(\frac{\gamma_2 - \gamma_1}{2}\right)} \tag{A1}$$

and the world coordinates are

$$z_w = d \sin\left(\frac{\gamma_1 + \gamma_2}{2}\right) \tag{A2}$$

$$y_w = d \cos\left(\frac{\gamma_1 + \gamma_2}{2}\right) \sin \phi \tag{A3}$$

$$x_w = d \cos\left(\frac{\gamma_1 + \gamma_2}{2}\right) \cos \phi \tag{A4}$$

No measurements were made to ascertain the accuracy of this measurement technique.

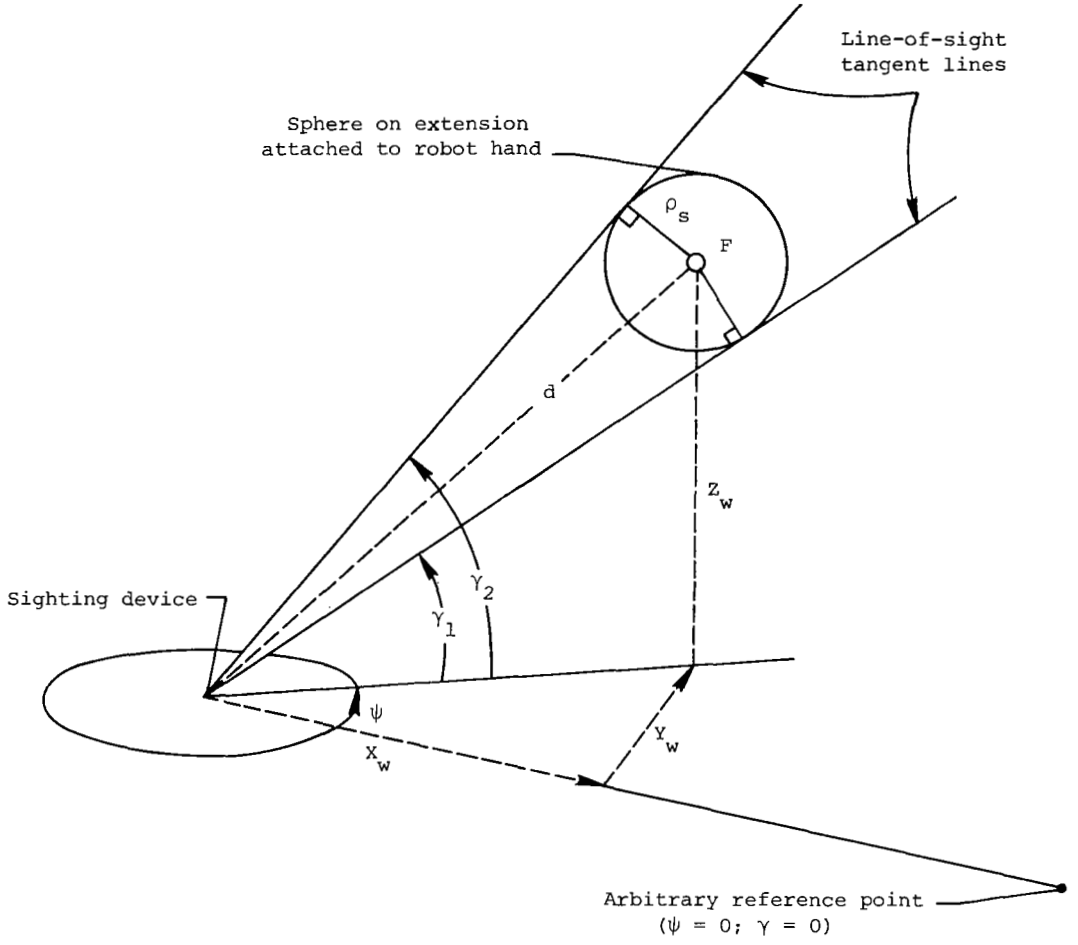

Figure A1.- Using sighting device to obtain world coordinates (x_w, y_w, z_w) of point F located at center of sphere being held by robot hand.

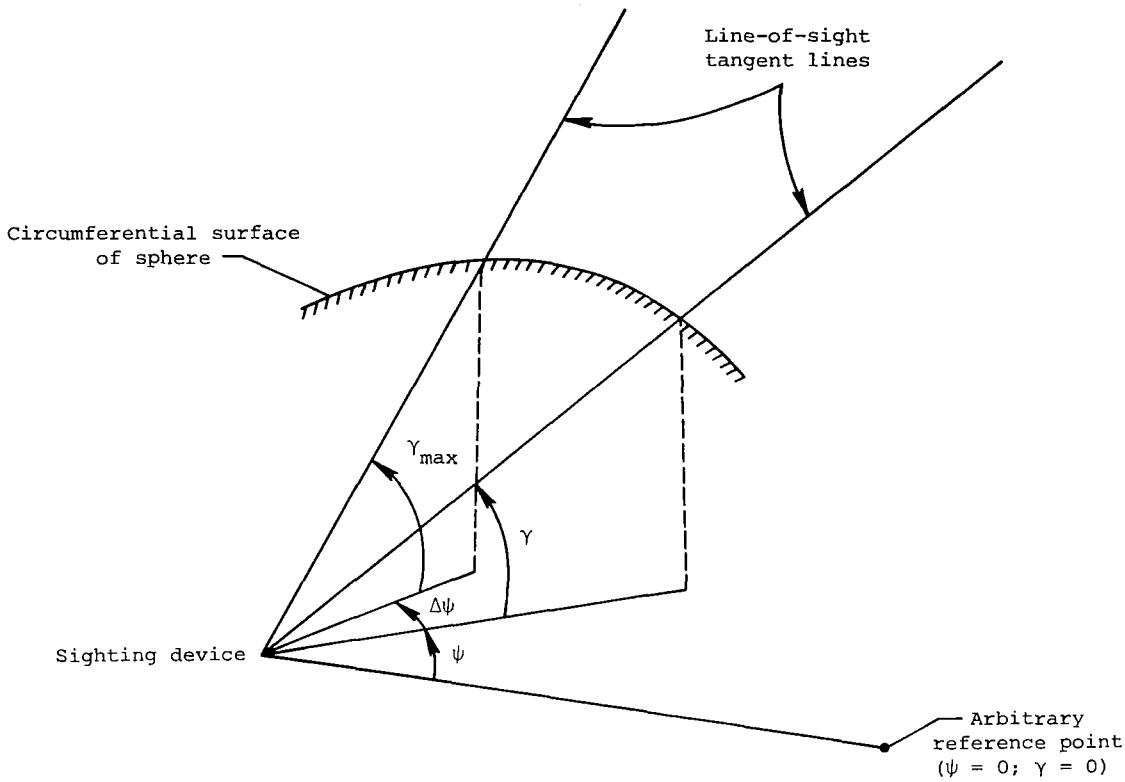

Figure A2.- Illustration of maximum elevation angle for line-of-sight tangent line to spherical surface.

APPENDIX B

RELATIVE JOINT GEOMETRY FOR SLIDING JOINTS

In the text, primary emphasis is placed on rotational joints; however, the same basic analysis holds for sliding joints (extendable segments). Let $\vec{r}_{i+1}$ be the extension variable and θ_{i+1} be a constant for joint $i + 1$ in the robot arm. Measuring locations of a point F on the robot arm for two different extensions ($\vec{r}_{i+1}(k)$, where $k = 1$ and 2) gives two points on a line. Let $\vec{P}_{i+1}(1)$ correspond to the extension $\vec{r}_{i+1} = \vec{r}_{i+1}(1)$ and $\vec{P}_{i+1}(2)$ correspond to $\vec{r}_{i+1} = \vec{r}_{i+1}(2)$, where $\|\vec{r}_{i+1}(2)\| > \|\vec{r}_{i+1}(1)\|$. Then, instead of the unit vector in equation (9), the unit vector is

$$\vec{u}_{i+1} = \frac{\vec{P}_{i+1}(2) - \vec{P}_{i+1}(1)}{\|\vec{P}_{i+1}(2) - \vec{P}_{i+1}(1)\|} \tag{B1}$$

Furthermore, instead of the line equation (12), the new line equation is

$$\vec{\ell}_{i+1} = \vec{P}_{i+1}(1) + \lambda_{i+1}\,\vec{u}_{i+1} \tag{B2}$$

The remaining steps in the parameter extraction are the same as in the text.

The line of extension represented by equation (B2) can be shifted, if desired, to pass through some chosen point; for example, the $\vec{P}_{i+1}(1)$ in the equation can be replaced by $\vec{R}_{i-1}$. This makes the a_i terms in equation (2) equal to zero for sliding joints (ref. 5).

REFERENCES

1. Meintel, Alfred J., Jr.; and Larsen, Ronald L.: NASA Research in Teleoperation and Robotics. Paper presented at Society of Photo-Optical Instrumentation Engineers Conference (San Diego, California), Aug. 23-27, 1982.

2. Whitney, Daniel E.: Resolved Motion Rate Control of Manipulators and Human Prostheses. IEEE Trans. Man-Mach. Sys., vol. MMS-10, no. 2, June 1969, pp. 47-53.

3. Denavit, J.; and Hartenberg, R. S.: A Kinematic Notation for Lower-Pair Mechanisms Based on Matrices. J. Appl. Mech., vol. 22, no. 2, June 1955, pp. 215-221.

4. Yeh, Shao-Chi: Locomotion of a Three-Legged Robot Over Structural Beams. M.S. Thesis, The Ohio State Univ., Aug. 1981.

5. Paul, Richard P.: Robot Manipulators: Mathematics, Programming, and Control - The Computer Control of Robot Manipulators. MIT Press, 1982.

TABLE I.- DIRECTION OF X_i

Consecutive lines of rotation	$\|\vec{u}_i \times \vec{u}_{i+1}\|$	$\|\vec{a}_i\|$	Direction of X_i
Do not intersect and not parallel	$\neq 0$	$\neq 0$	Either $\vec{u}_i \times \vec{u}_{i+1}$ or $\vec{a}_i$
Intersect but not parallel	$\neq 0$	0	$\vec{u}_i \times \vec{u}_{i+1}$
Parallel but separated	0	$\neq 0$	$\vec{a}_i$
Coincident lines are excluded	0	0	Excluded

TABLE II.- CONSISTENT TANGENT EQUATIONS FOR α_i AND θ_i'

Direction of current X_i	Previously defined direction of X_{i-1}	
	$\vec{u}_{i-1} \times \vec{u}_i$	$\vec{a}_{i-1}$
$\vec{u}_i \times \vec{u}_{i+1}$	$\tan \theta_i' = \dfrac{[(\vec{u}_{i-1} \times \vec{u}_i) \times (\vec{u}_i \times \vec{u}_{i+1})] \cdot \vec{u}_i}{(\vec{u}_{i-1} \times \vec{u}_i) \cdot (\vec{u}_i \times \vec{u}_{i+1})}$ $\tan \alpha_i = \dfrac{\lVert \vec{u}_i \times \vec{u}_{i+1} \rVert}{\vec{u}_i \cdot \vec{u}_{i+1}}$	$\tan \theta_i' = \dfrac{[\vec{a}_{i-1} \times (\vec{u}_i \times \vec{u}_{i+1})] \cdot \vec{u}_i}{\vec{a}_{i-1} \cdot (\vec{u}_i \times \vec{u}_{i+1})}$ $\tan \alpha_i = \dfrac{\lVert \vec{u}_i \times \vec{u}_{i+1} \rVert}{\vec{u}_i \cdot \vec{u}_{i+1}}$
$\vec{a}_i$	$\tan \theta_i' = \dfrac{[(\vec{u}_{i-1} \times \vec{u}_i) \times \vec{a}_i] \cdot \vec{u}_i}{(\vec{u}_{i-1} \times \vec{u}_i) \cdot \vec{a}_i}$ $\tan \alpha_i = \left[(\vec{u}_i \times \vec{u}_{i+1}) \cdot \dfrac{\vec{a}_i}{\lVert \vec{a}_i \rVert} \right] \Big/ \vec{u}_i \cdot \vec{u}_{i+1}$	$\tan \theta_i' = \dfrac{(\vec{a}_{i-1} \times \vec{a}_i) \cdot \vec{u}_i}{\vec{a}_{i-1} \cdot \vec{a}_i}$ $\tan \alpha_i = \left[(\vec{u}_i \times \vec{u}_{i+1}) \cdot \dfrac{\vec{a}_i}{\lVert \vec{a}_i \rVert} \right] \Big/ \vec{u}_i \cdot \vec{u}_{i+1}$

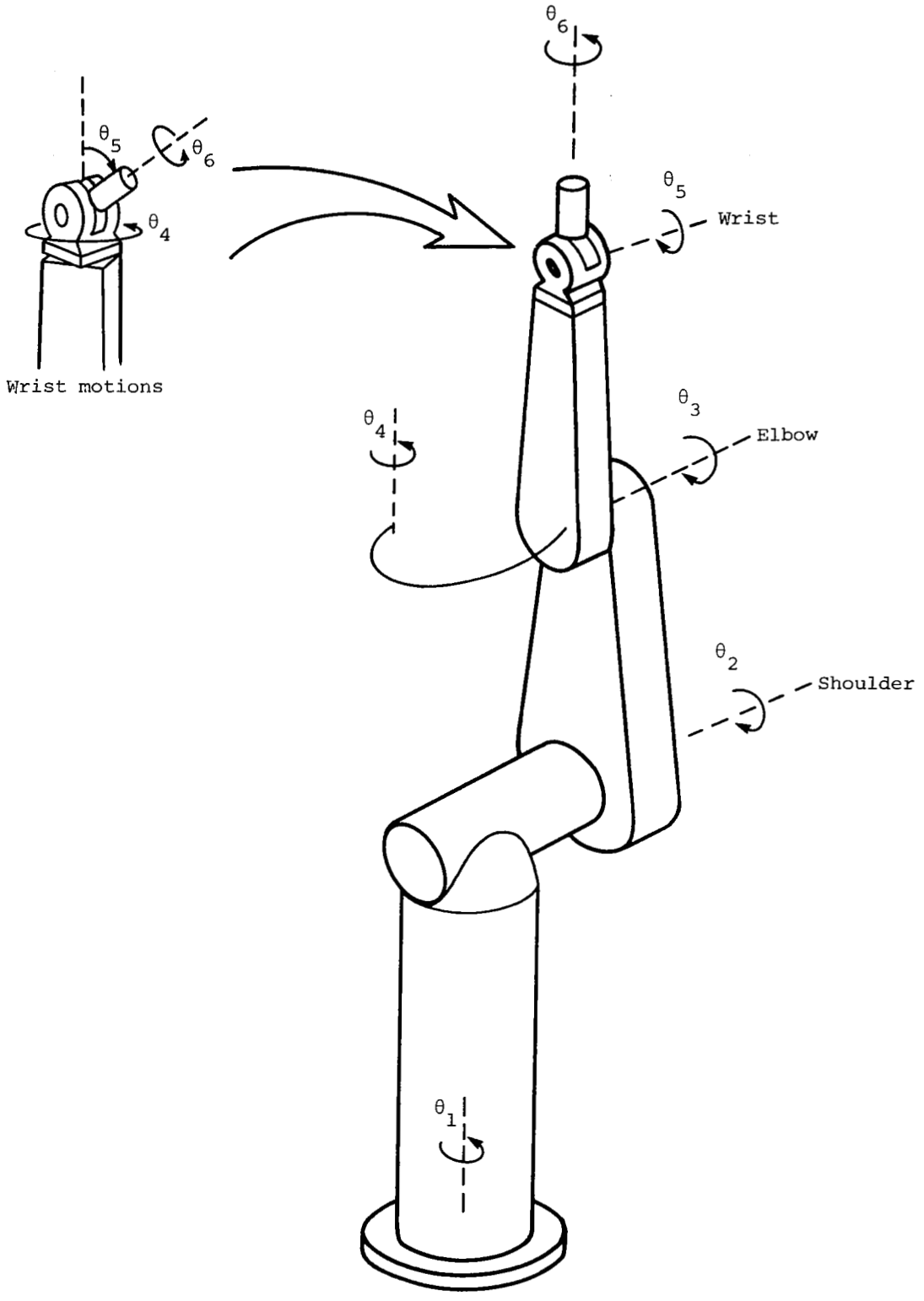

Figure 1.- Robot arm with rotational joints. Initial position.

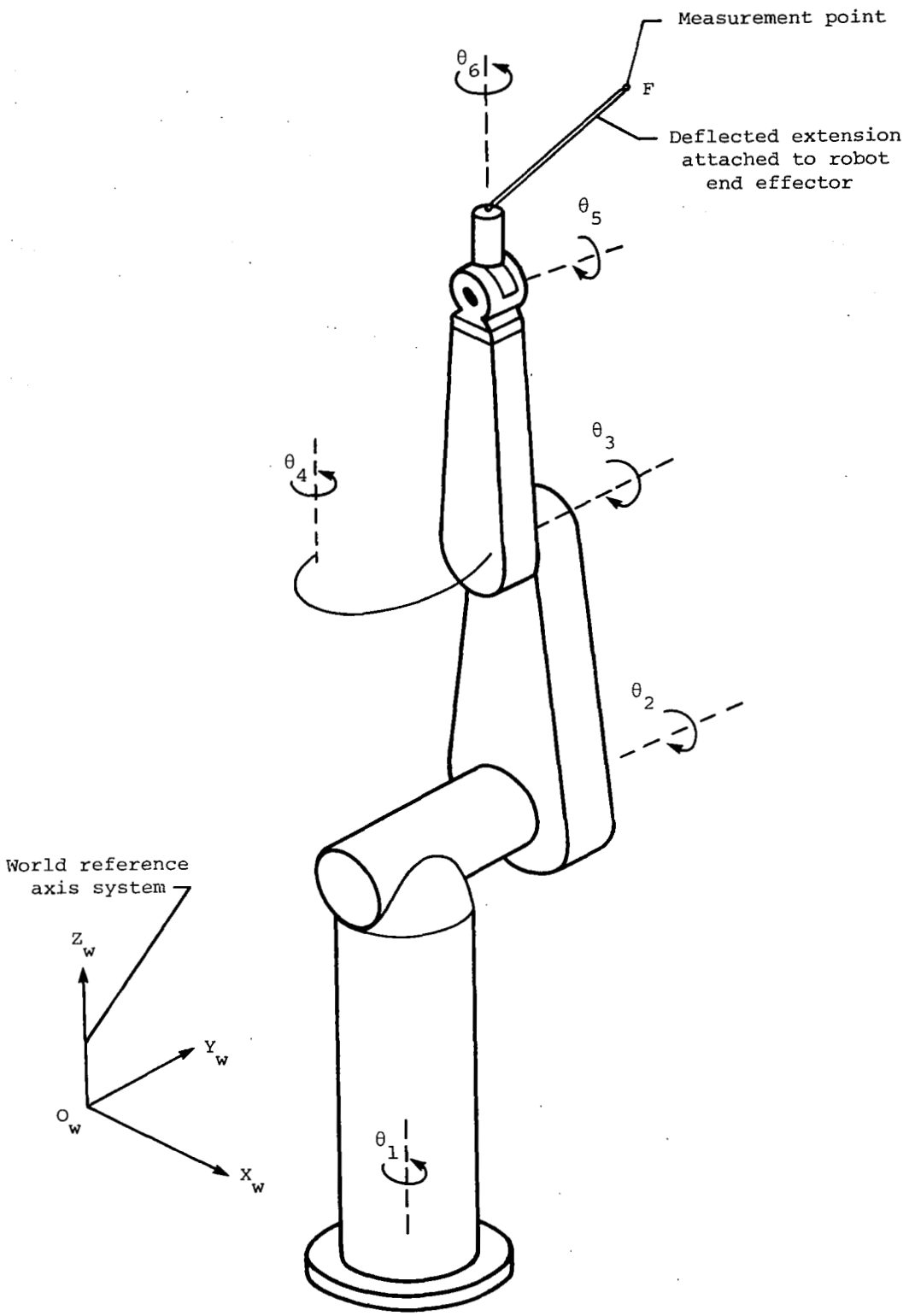

Figure 2.- World axis system and robot arm with extension for measurements.

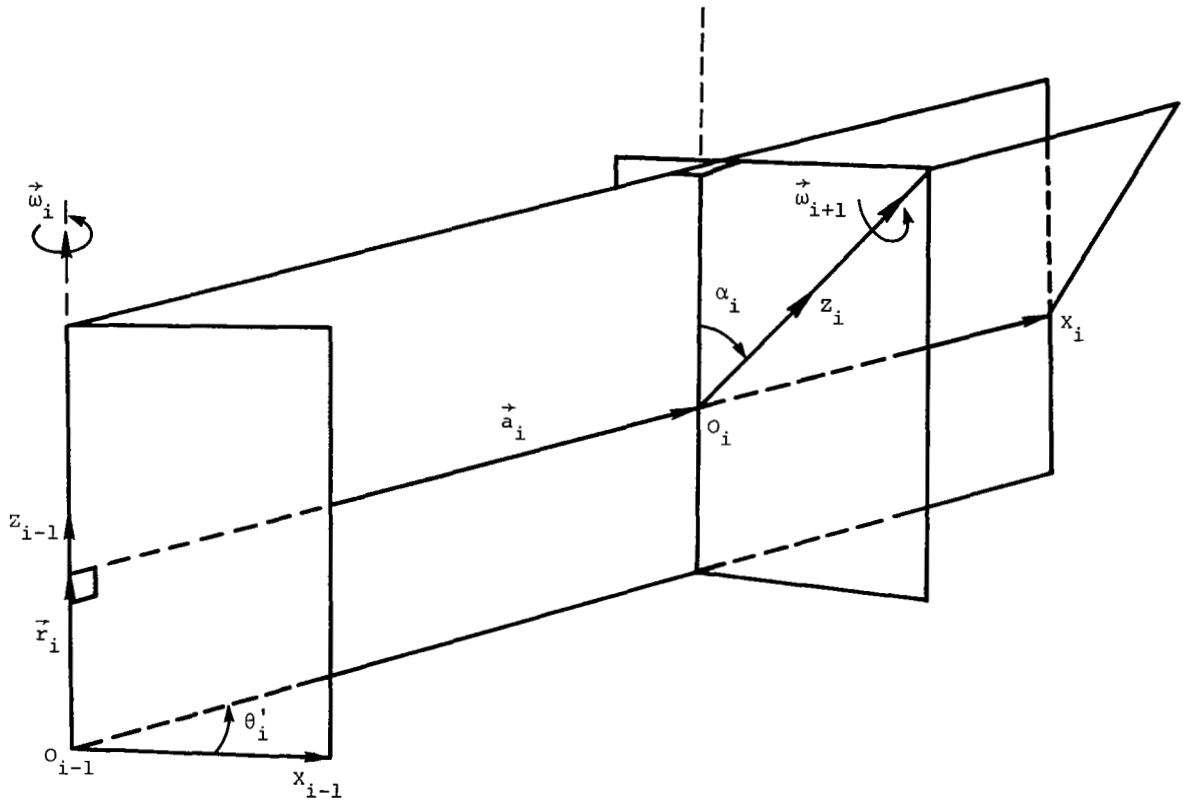

(a) Nonintersecting lines of rotation.

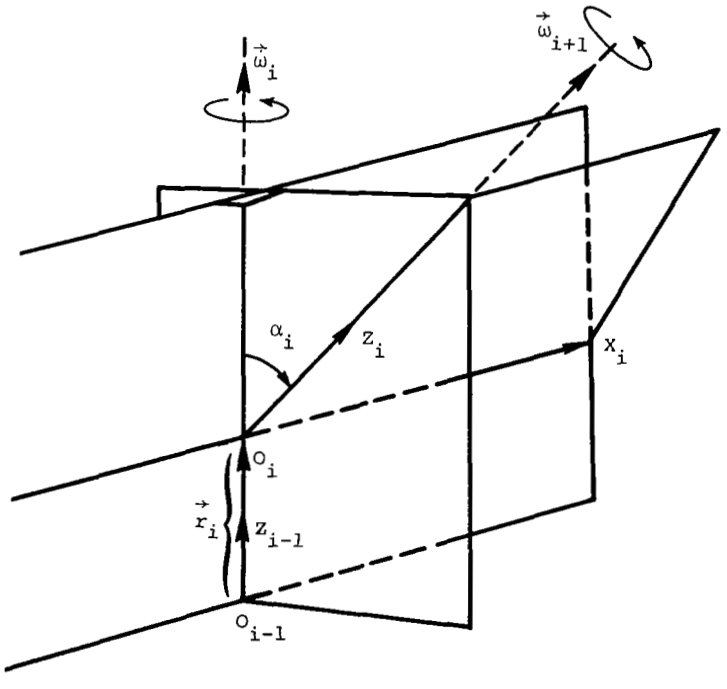

(b) Intersecting lines of rotation.

Figure 3.- Consecutive joint axis systems and relative joint geometry.

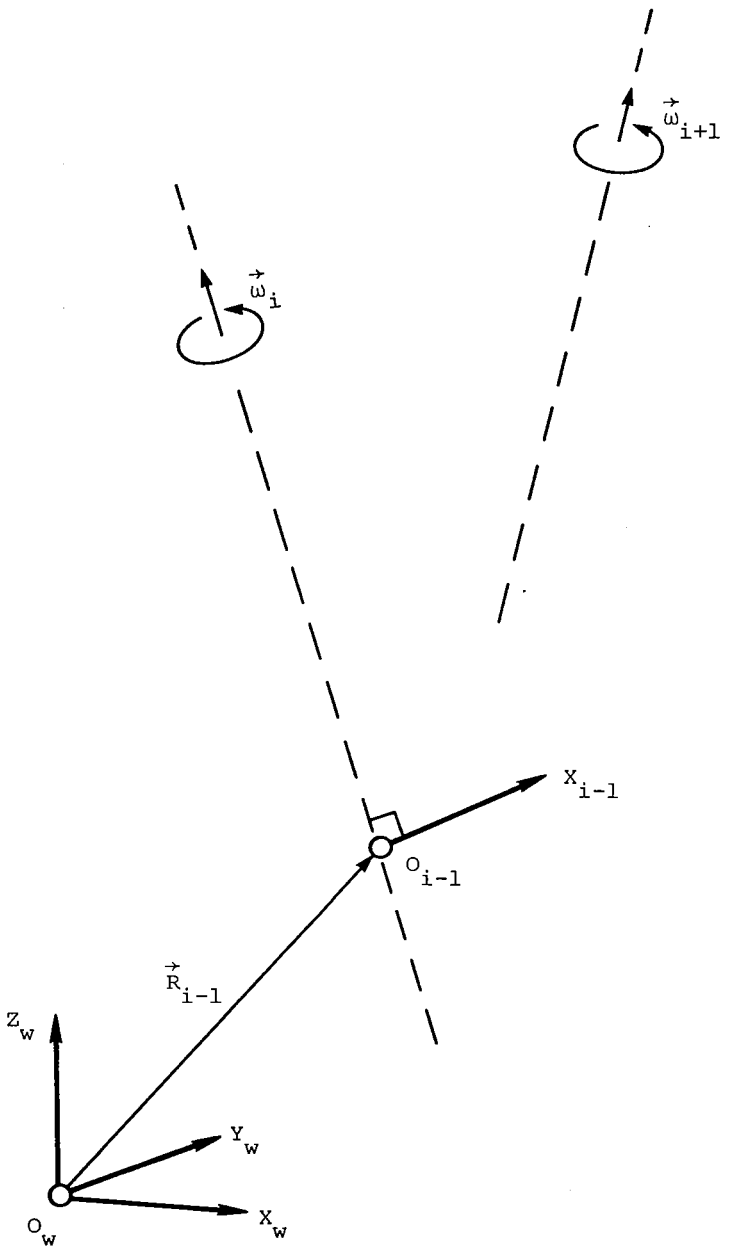

Figure 4.- Illustration of world axis system, vector $\vec{R}_{i-1}$, and direction of X_{i-1} for problem statement. Dashed lines represent unknown lines of rotation for consecutive joints.

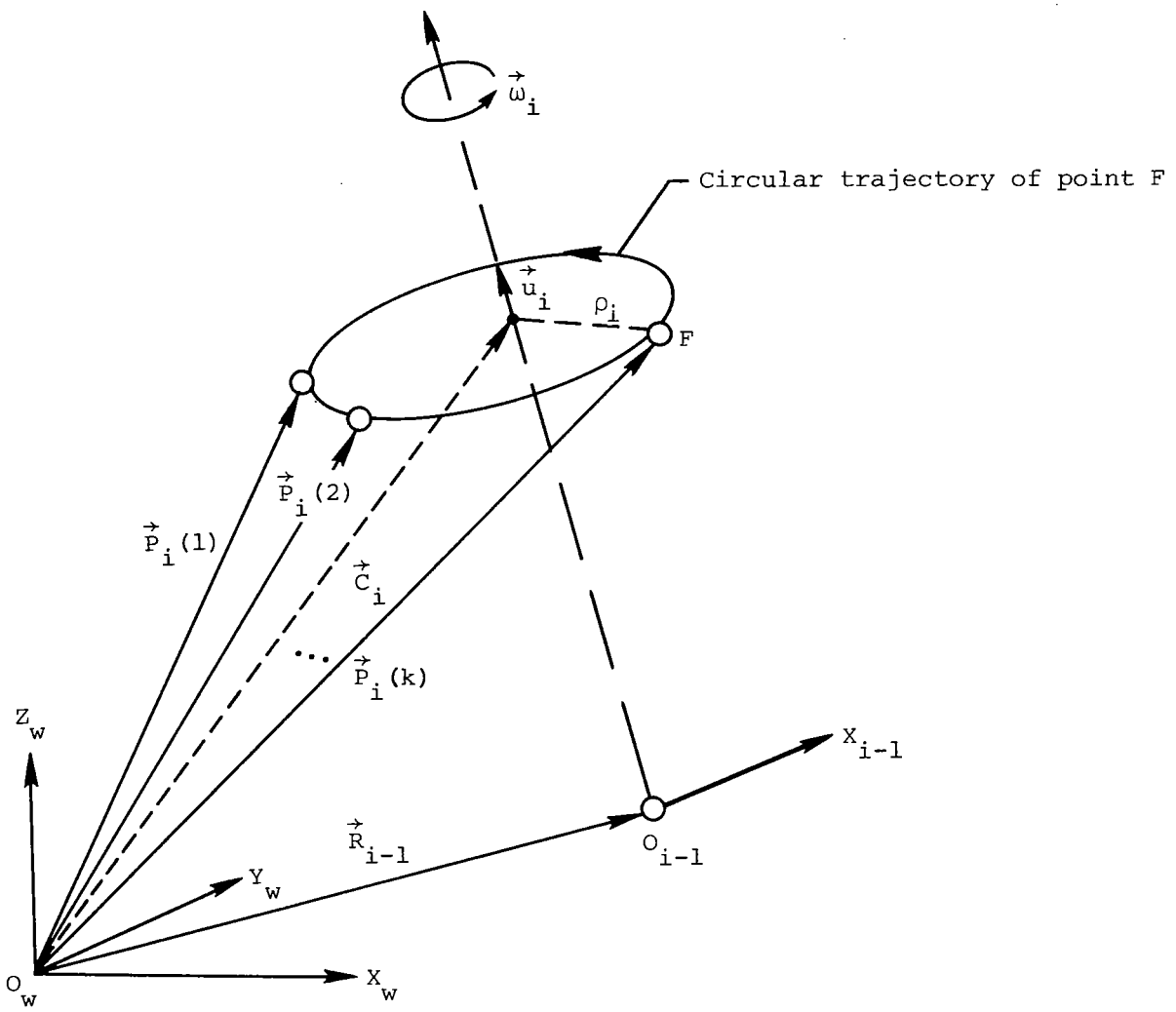

Figure 5.- Circular trajectory of point F about line of rotation for joint i.

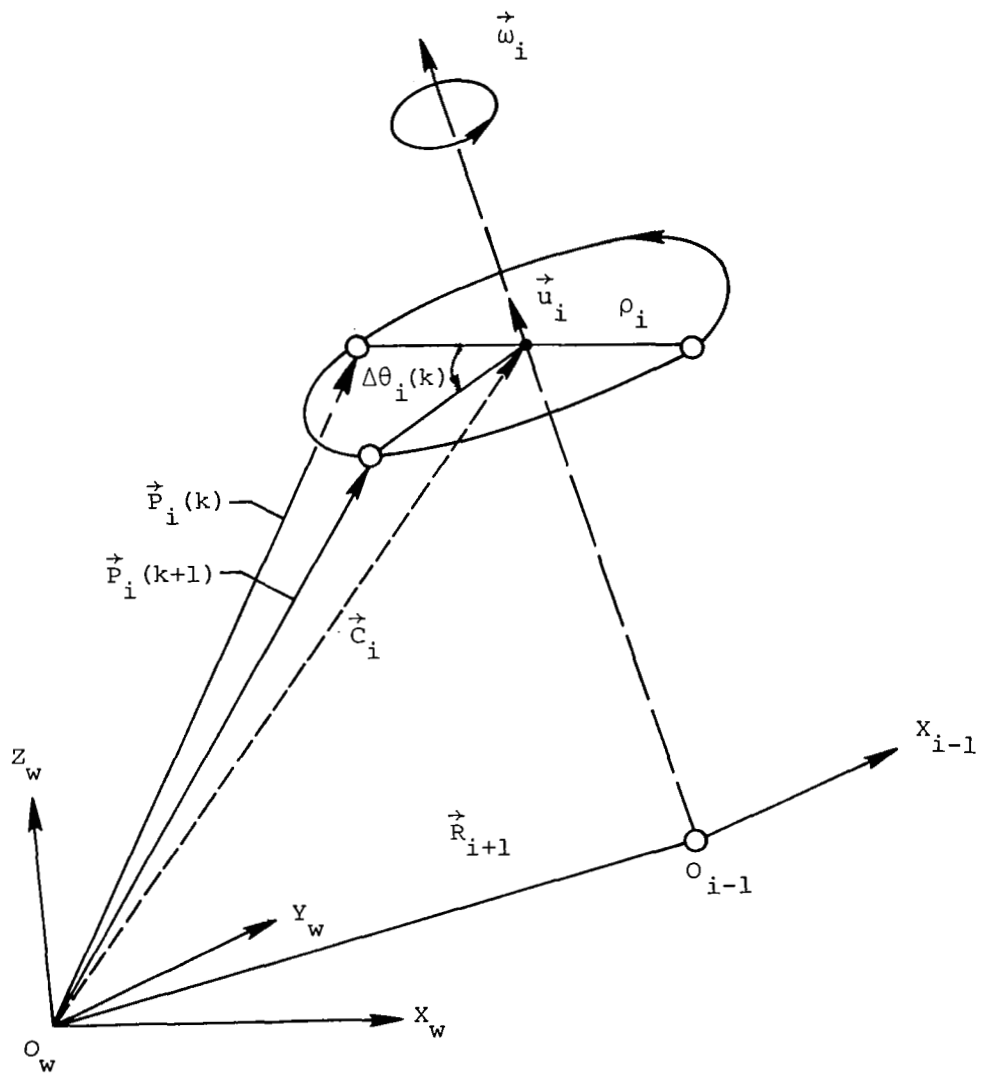

Figure 6.- Unit vector in same direction as joint rotational vector.

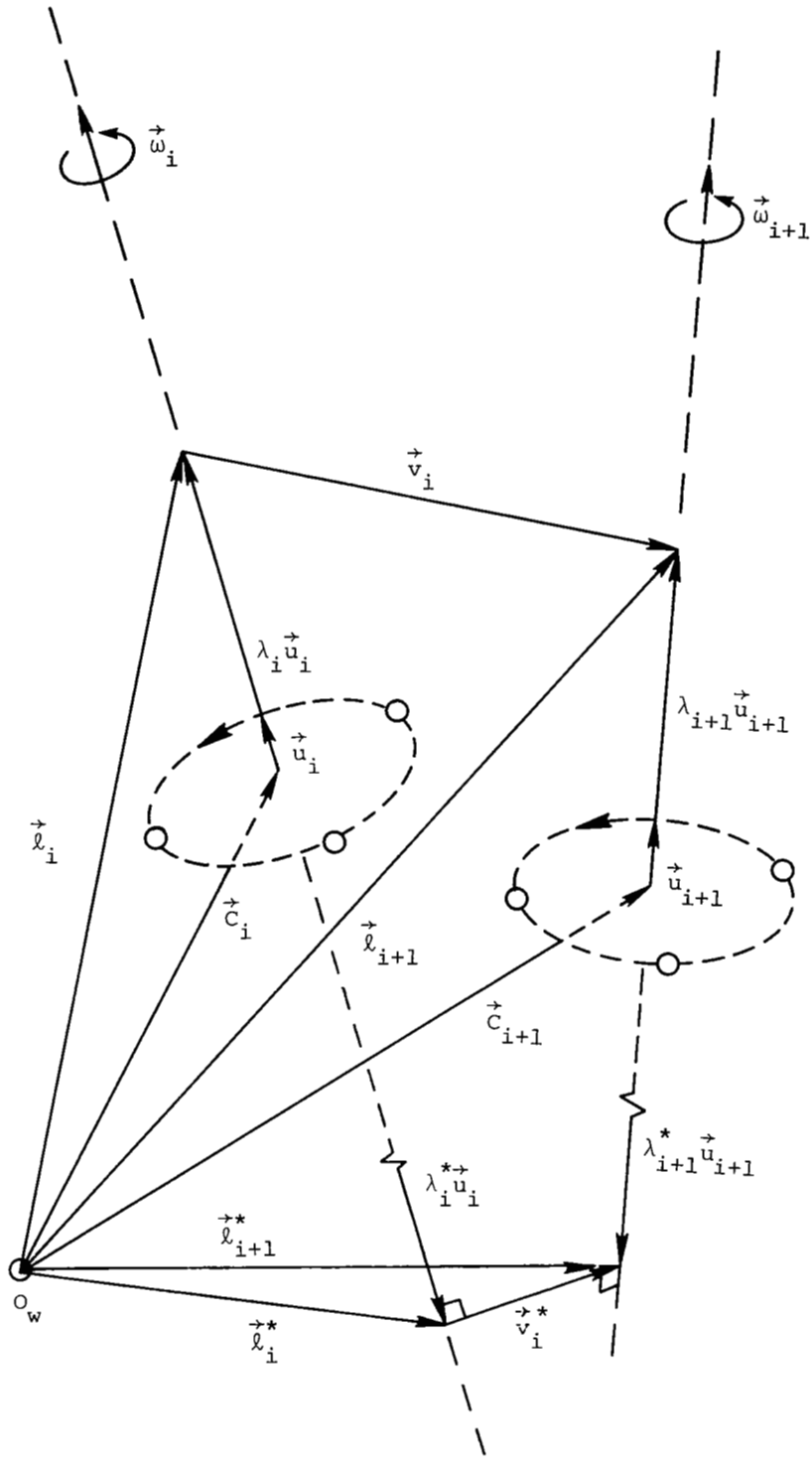

Figure 7.- Lines of rotation for consecutive joints and transverse vector.

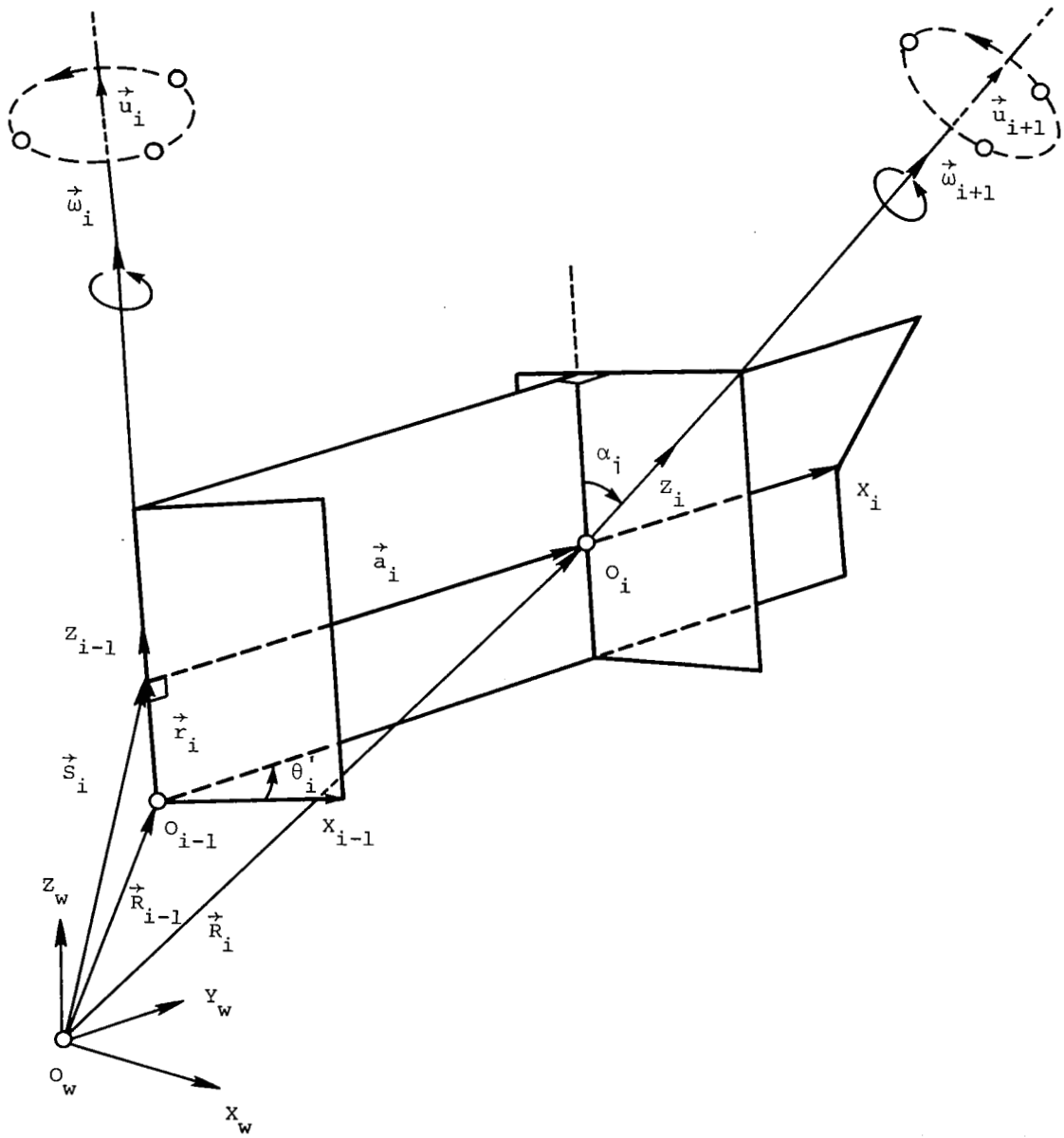

Figure 8.- Composite figure showing geometry involved in parameter-extraction method.

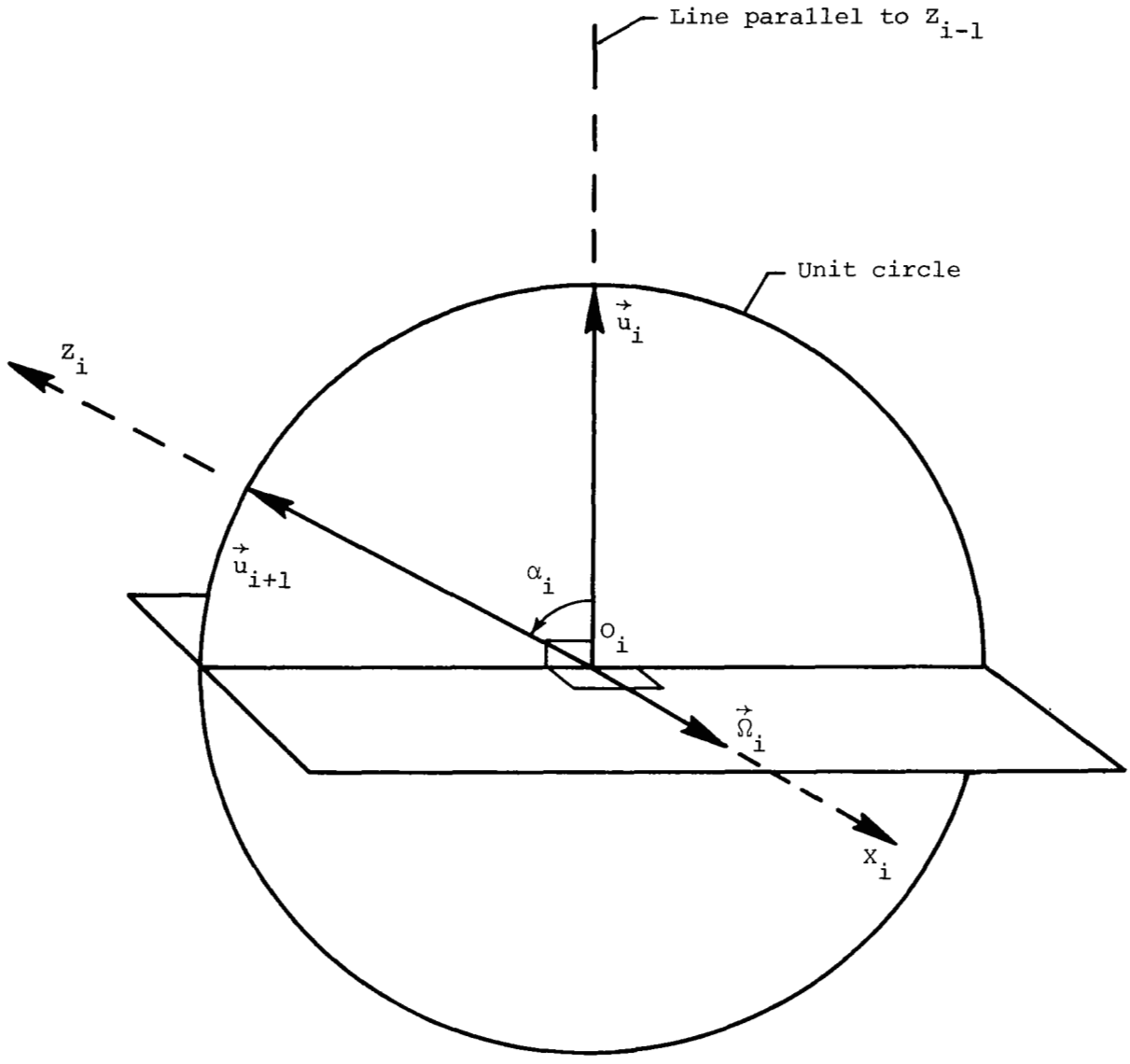

Figure 9.- Geometry illustrating X_i defined in direction of $\vec{u}_i \times \vec{u}_{i+1}$.

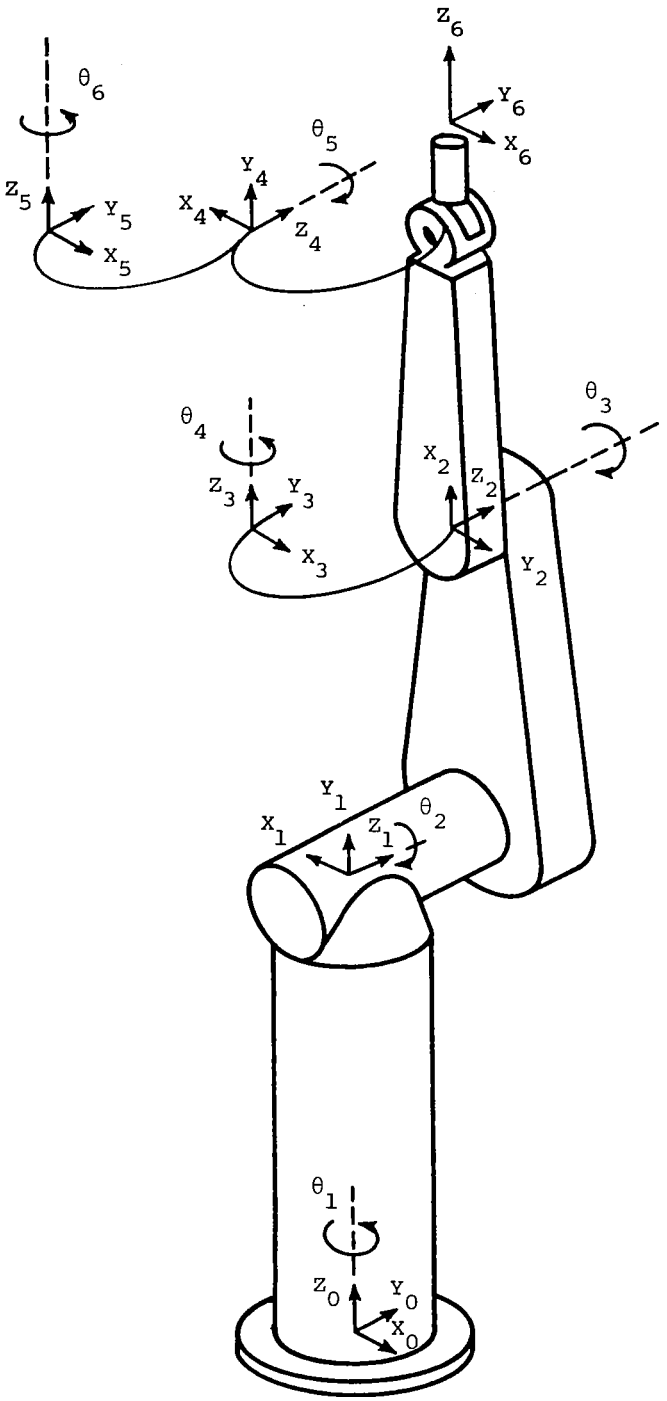

Figure 10.- Robot arm with axis systems.

1. Report No.	2. Government Accession No.	3. Recipient's Catalog No.
NASA TP-2191		

4. Title and Subtitle	5. Report Date
VECTOR-ALGEBRA APPROACH TO EXTRACT DENAVIT-HARTENBERG PARAMETERS OF ASSEMBLED ROBOT ARMS	August 1983
	6. Performing Organization Code: 506-54-63-01-00
7. Author(s): L. Keith Barker	8. Performing Organization Report No.: L-15621
	10. Work Unit No.
9. Performing Organization Name and Address: NASA Langley Research Center, Hampton, VA 23665	11. Contract or Grant No.
	13. Type of Report and Period Covered: Technical Paper
12. Sponsoring Agency Name and Address: National Aeronautics and Space Administration, Washington, DC 20546	14. Sponsoring Agency Code

15. Supplementary Notes

16. Abstract

The Denavit-Hartenberg parameters characterize the joint axis systems in a robot arm and, naturally, appear in the transformation matrices from one joint axis system to another. These parameters are needed in the control of robot arms and in the passage of sensor information along the arm. This paper presents a vector-algebra method to determine these parameters for any assembled robot arm. The idea is to measure the location of the robot hand (or extension) for different joint angles and then use these measurements to calculate the parameters.

17. Key Words (Suggested by Author(s))	18. Distribution Statement
Robot arm Manipulator Denavit-Hartenberg parameters Joint axis systems Relative joint geometry Parameter extraction	Unclassified - Unlimited Subject Category 64

19. Security Classif. (of this report)	20. Security Classif. (of this page)	21. No. of Pages	22. Price
Unclassified	Unclassified	32	A03

For sale by the National Technical Information Service, Springfield, Virginia 22161

NASA-Langley, 1983